Examination of the observability of a chiral magnetically driven charge-separation difference in collisions of the _{44}^{96}Ru+_{44}^{96}Ru and _{40}^{96}Zr+_{40}^{96}Zr isobars at energies available at the BNL Relativistic Heavy Ion Collider

Niseem Magdy, Shuzhe Shi, Jinfeng Liao, Peifeng Liu, and Roy A. Lacey

Phys. Rev. C **98**, 061902 — Published 19 December 2018

DOI: 10.1103/PhysRevC.98.061902

Examination of the observability of a chiral magnetically-driven charge-separation difference in collisions of the $^{96}_{44}$Ru + $^{96}_{44}$Ru and $^{96}_{40}$Zr + $^{96}_{40}$Zr isobars at energies available at the BNL Relativistic Heavy Ion Collider

Niseem Magdy,[1] Shuzhe Shi,[2] Jinfeng Liao,[2,*] Peifeng Liu,[1,3] and Roy A. Lacey[1,3,†]

[1] *Department of Chemistry, Stony Brook University, Stony Brook, New York 11794, USA*
[2] *Physics Department and Center for Exploration of Energy and Matter, Indiana University, 2401 N Milo B. Sampson Lane, Bloomington, IN 47408, USA.*
[3] *Department of Physics, Stony Brook University, Stony Brook, New York 11794, USA*

(Dated: December 2, 2018)

Anomalous Viscous Fluid Dynamics (AVFD) model calculations for $^{96}_{44}$Ru + $^{96}_{44}$Ru and $^{96}_{40}$Zr + $^{96}_{40}$Zr collisions ($\sqrt{s_{\rm NN}}$ = 200 GeV) are used in concert with a charge-sensitive correlator, to test its ability to detect and characterize the charge separation difference expected from the Chiral Magnetic Effect (CME) in these isobaric collisions. The tests indicate a larger charge separation for $^{96}_{44}$Ru + $^{96}_{44}$Ru than for $^{96}_{40}$Zr + $^{96}_{40}$Zr collisions, and a discernible CME-driven difference of $\sim 10\%$ in the presence of realistic non-CME backgrounds. They also indicate a strategy for evaluating the relative influence of the background correlations, present for each isobar. These results suggest that charge separation measurements for these isobaric species, could serve to further constrain unambiguous identification and characterization of the CME in upcoming measurements at RHIC.

PACS numbers: 25.75.-q, 25.75.Gz, 25.75.Ld

Isobaric collisions of $^{96}_{44}$Ru + $^{96}_{44}$Ru and $^{96}_{40}$Zr + $^{96}_{40}$Zr at $\sqrt{s_{\rm NN}}$ = 200 GeV, will be used in an upcoming experiment at the Relativistic Heavy Ion Collider (RHIC) to measure and characterize a possible charge separation difference, induced by the Chiral Magnetic Effect (CME) in these collisions [1, 2]. Experimental validation of this purported signal, would constitute an invaluable constraint to further identify and characterize the CME in heavy ion collisions. In addition, it could provide crucial insight on anomalous transport and the interplay of chiral symmetry restoration, axial anomaly, and gluonic topology in the QGP.

The rationale for the isobaric collision experiment, stems from two invaluable considerations. The first is that, by choosing isobars, the well known background correlations which complicate charge separation measurements [3–8] are made similar, and this greatly facilitates a comparison of the measurements for both systems. The second is the expectation that the net axial-charge asymmetry of the chiral quarks in the quark-gluon plasma (QGP) [9, 10] created in the isobaric collisions, are similar, but the time-dependent electromagnetic $\vec{B}$ fields [11–13] produced for similar impact parameter, is larger for $^{96}_{44}$Ru + $^{96}_{44}$Ru, due to its larger charge to mass ratio. Thus, the chiral anomaly for $^{96}_{44}$Ru + $^{96}_{44}$Ru should convert into a stronger electric current than for $^{96}_{40}$Zr + $^{96}_{40}$Zr,

$$\vec{J}_Q = \sigma_5 \vec{B}, \quad \sigma_5 = \mu_5 \frac{Q^2}{4\pi^2}, \tag{1}$$

leading to a larger final-state charge separation perpendicular to the reaction plane ($\Psi_{\rm RP}$) defined by the impact parameter and the beam axis [2, 14–19]; here, σ_5 is the chiral magnetic conductivity, μ_5 is the chiral chemical potential that quantifies the axial charge asymmetry or imbalance between right-handed and left-handed quarks in the plasma, and Q is the quark electric charge [17, 20–22].

Figure 1(a) shows a clear hierarchy in the magnitude of the peak magnetic field values $B_0 = \left\langle (\mathrm{eB})^2 \cos(2\Delta\Psi_{\rm B}^{\rm PP}) \right\rangle^{1/2}$, evaluated perpendicular to the respective participant planes $\Psi_{\rm B}^{\rm PP}$, in Au+Au, Ru+Ru and Zr+Zr collisions at $\sqrt{s_{\rm NN}}$ = 200 GeV; $\Delta\Psi_{\rm B}^{\rm PP}$ is the angle of the participant plane relative to $\Psi_{\rm RP}$, so the B_0 values take into account the $\vec{B}$-field fluctuations. The procedure employed to compute B_0 is akin to that employed in Ref. [23]. Figs.1(b) and (c) show that the ratio of these peak values scale approximately as the charge to mass ratio, and the magnetic field for $^{96}_{44}$Ru + $^{96}_{44}$Ru collisions is $\sim 8-10\%$ larger [24] than that for $^{96}_{40}$Zr + $^{96}_{40}$Zr collisions for the same centrality selection. Therefore, a major objective of the isobaric collision experiment, is to identify and quantify a CME-driven charge separation difference between $^{96}_{44}$Ru + $^{96}_{44}$Ru and $^{96}_{40}$Zr + $^{96}_{40}$Zr of order 10%, via measurements of the first P-odd sine term (a_1) in the Fourier decomposition of the charged-particle azimuthal distribution [25] for both systems:

$$\frac{\mathrm{dN^{ch}}}{\mathrm{d}\phi} \propto [1 + 2\sum_{\rm n} \mathrm{v_n}\cos(\mathrm{n}\Delta\phi) + \mathrm{a_n}\sin(\mathrm{n}\Delta\phi) + ...] \tag{2}$$

where $\Delta\phi = \phi - \Psi_{\rm RP}$ gives the particle azimuthal angle with respect to the reaction plane angle, and $\mathrm{v_n}$ and $\mathrm{a_n}$ denote the coefficients of P-even and P-odd Fourier terms, respectively. The second-order event plane, Ψ_2, determined by the maximal particle density in the elliptic azimuthal anisotropy and the beam axis, serves as a proxy for $\Psi_{\rm RP}$ in experimental measurements.

* liaoji@indiana.edu
† Roy.Lacey@stonybrook.edu

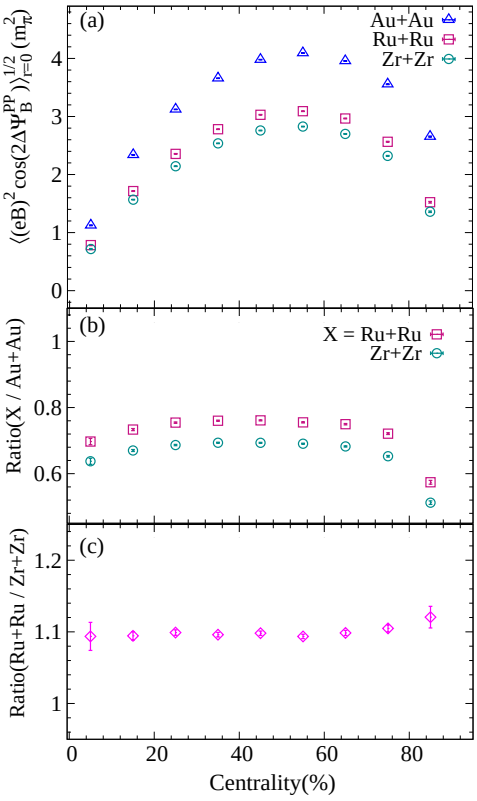

FIG. 1. (a) Comparison of the centrality dependence of the peak magnetic fields B_0 (perpendicular to the respective participant planes Ψ_B^{PP} which fluctuate about Ψ_{RP}), for Au+Au Ru+Ru and Zr+Zr collisions at $\sqrt{s_{NN}}$ = 200 GeV. Panels (b) and (c) show the the centrality dependence of the ratio of these peak magnetic fields [24].

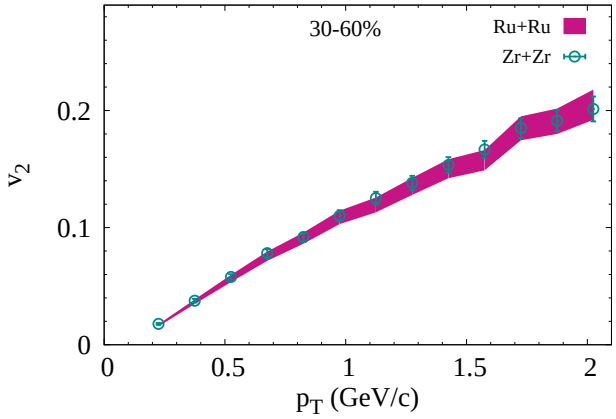

FIG. 2. Comparison of the differential elliptic flow $v_2(p_T)$, extracted from AVFD events for 30-60% central $^{96}_{44}$Ru + $^{96}_{44}$Ru and $^{96}_{40}$Zr + $^{96}_{40}$Zr collisions at $\sqrt{s_{NN}}$ = 200 GeV. The extractions were carried out for charged hadrons with $|\eta| \lesssim 1.5$ with the event planes constructed in the range $2.5 \lesssim |\eta| \lesssim 4.0$.

In addition to the B_0 difference indicated for the isobars, it is noteworthy that Fig. 1 also suggest a specific hierarchy, as well as patterns in the relative magnitudes for CME-driven charge separation for the systems indicated. The observation of such magnitudes and trends in future charge separation measurements could also serve as an important constraint.

A caveat on the proposed measurement for the isobars, is that the initial axial charge and the time evolution of the magnetic field (c.f. Eq. 1) are unconstrained theoretically. Thus, it is not certain whether the expected $\vec{B}$-driven charge separation difference would remain detectable, after possible signal losses associated with the dynamics of the evolution from the QGP phase to particle freeze-out. It is also uncertain whether a charge separation difference that survives the reaction dynamics, would still be discernible in the presence of the well known background correlations which contribute and complicate the measurement of CME-driven charge separation [3–8].

In recent work [26], we have developed and tested a new correlator designed to give discernible responses for background- and CME-driven charge separation relative to the Ψ_3 and Ψ_2 event planes respectively. An initial rudimentary comparison of the correlators for preliminary data [27] and theory, indicated results compatible with a CME-driven charge separation in 40-50% central Au+Au collisions at $\sqrt{s_{NN}}$ = 200 GeV. Here, we use this correlator in concert with state-of-the-art Anomalous Viscous Fluid Dynamics (AVFD) model calculations, to test its efficacy to detect and characterize the expected charge separation difference, induced by the Chiral Magnetic Effect (CME), in $^{96}_{44}$Ru + $^{96}_{44}$Ru and $^{96}_{40}$Zr + $^{96}_{40}$Zr collisions. The tests are performed under "realistic" AVFD model conditions, which mimic the complications that could result from the influence of both the reaction dynamics and background correlations.

The AVFD model [19, 28] uses Monte Carlo Glauber initial conditions to simulate the evolution of fermion currents in the QGP, on top of the bulk fluid evolution implemented in the VISHNU hydrodynamic code [29], supplemented with a URQMD hadron cascade "afterburner" stage. The code gives a good representation of the experimentally measured bulk properties – particle yields, spectra, flow, etc. Therefore, it gives a realistic estimate of the magnitude and trends of the background correlations expected in the isobaric data samples to be obtained at RHIC. Fig. 2 shows that the AVFD values for elliptic flow ($v_2(p_T)$), a major driver of background correlations, is similar for the two isobars and is in line with expectation that the background correlations for $^{96}_{44}$Ru + $^{96}_{44}$Ru and $^{96}_{40}$Zr + $^{96}_{40}$Zr should be similar for the indicated centrality range [2, 30]. The two isobars have a small deformation difference which leads to eccentricity (ε_2) differences and consequently, a v_2 differences for centralities $\lesssim 30\%$ [30]. However, such a difference would not have a strong impact on our analysis as discussed below.

Anomalous transport from the CME, is also implemented in the AVFD model. This is accomplished via a time-dependent magnetic field $B(\tau) = \frac{B_0}{1+(\tau/\tau_B)^2}$, which acts in concert with a nonzero initial axial charge density, to generate a CME current (encoded in the fluid dynamical equations). The peak values B_0, of the magnetic field, is obtained from event-by-event simulations [31], and are used with a relatively conservative lifetime $\tau_B = 0.6$ fm/c, to generate the time-dependence of the magnetic field. The estimate for the initial axial charge density, which results from gluonic topological charge fluctuations, is based on the strong chromo-electromagnetic fields developed in the early-stage glasma phase [10, 32].

With these essential ingredients, the AVFD model was used to simulate a charge separation along the $\vec{B}$-field (i.e. perpendicular to the reaction plane), in combination with background correlations, for $^{96}_{44}$Ru + $^{96}_{44}$Ru and $^{96}_{40}$Zr + $^{96}_{40}$Zr collisions at $\sqrt{s_{\rm NN}} = 200$ GeV. A subsequent analysis of these simulated events was performed to identify and quantify the predicted CME-driven charge separation difference between the two isobars.

The correlator $R_{\Psi_2}(\Delta S)$, constructed relative to the Ψ_2 plane, was used for the charge separation measurements. As outlined in Ref. [26], the correlators $R_{\Psi_m}(\Delta S)$ can be expressed as the ratios:

$$R_{\Psi_m}(\Delta S) = C_{\Psi_m}(\Delta S)/C^{\perp}_{\Psi_m}(\Delta S),\ m = 2, 3, \quad (3)$$

where $C_{\Psi_m}(\Delta S)$ and $C^{\perp}_{\Psi_m}(\Delta S)$ are correlation functions designed to quantify charge separation ΔS, parallel and perpendicular (respectively) to the $\vec{B}$ field, i.e., perpendicular and parallel (respectively) to $\Psi_{\rm RP}$. The correlation function $C_{\Psi_2}(\Delta S)$ measures both CME- and background-driven charge separation, while $C^{\perp}_{\Psi_2}(\Delta S)$ measures only background-driven charge separation. The $C_{\Psi_3}(\Delta S)$ and $C^{\perp}_{\Psi_3}(\Delta S)$ correlation functions can also be used to provide insight on the importance of background-driven charge separation, because they are both insensitive to a CME-driven charge separation [26]. However, they are not essential for the present analysis, as will be shown below.

The $C_{\Psi_2}(\Delta S)$ correlation function, used to quantify charge separation parallel to the $\vec{B}$ field, is constructed from the ratio of two distributions [33]:

$$C_{\Psi_2}(\Delta S) = \frac{N_{\rm real}(\Delta S)}{N_{\rm Shuffled}(\Delta S)}, \quad (4)$$

where $N_{\rm real}(\Delta S)$ is the distribution over events, of charge separation relative to the Ψ_2 plane in each event:

$$\Delta S = \frac{\sum_1^p \sin(\frac{m}{2}\Delta\varphi_m)}{p} - \frac{\sum_1^n \sin(\frac{m}{2}\Delta\varphi_m)}{n}, \quad (5)$$

where n and p are the numbers of negatively- and positively charged hadrons in an event, $\Delta\varphi_2 = \phi - \Psi_2$ and ϕ is the azimuthal emission angle of the charged hadrons. The $N_{\rm Shuffled}(\Delta S)$ distribution was similarly obtained from the same events, following random reassignment (shuffling) of the charge of each particle in an event. This procedure ensures identical properties for the numerator and the denominator in Eq. 4, except for the charge-dependent correlations which are of interest.

The correlation function $C^{\perp}_{\Psi_2}(\Delta S)$, used to quantify charge separation perpendicular to the $\vec{B}$ field, i.e., background-driven charge separation, was constructed with the same procedure outlined for $C_{\Psi_2}(\Delta S)$, but with Ψ_2 replaced by $\Psi_2 + \pi/2$. This $\pi/2$ rotation of the event plane, suppresses the contributions from CME-driven charge separation to this correlation function.

The correlator $R_{\Psi_2}(\Delta S) = C_{\Psi_2}(\Delta S)/C^{\perp}_{\Psi_2}(\Delta S)$, gives a measure of the magnitude of charge separation parallel to the $\vec{B}$ field (perpendicular to Ψ_2), relative to that for charge separation perpendicular to the $\vec{B}$ field (parallel to Ψ_2). Consequently, correlations dominated by CME-driven charge separation are expected to result in a concave-shaped distributions with widths that are larger for $^{96}_{40}$Zr + $^{96}_{40}$Zr than for $^{96}_{44}$Ru + $^{96}_{44}$Ru. That is, the stronger CME-driven charge separation expected for $^{96}_{44}$Ru + $^{96}_{44}$Ru collisions, should lead to a narrower $R_{\Psi_2}(\Delta S)$ distribution. Here, it is noteworthy that the absence of a strong correlation between the orientation of the Ψ_3 plane and the $\vec{B}$-field, makes $R_{\Psi_3}(\Delta S)$ insensitive to the CME signal, but sensitive to background-driven charge separation. Thus, a background-driven charge separation would lead to similar patterns for the $R_{\Psi_2}(\Delta S)$ and $R_{\Psi_3}(\Delta S)$ correlators, while a CME-driven charge separation would result in characteristically different patterns for the two correlators.

The magnitude of a CME-driven charge separation is reflected in the width of the concave-shaped distribution for $R_{\Psi_2}(\Delta S)$ [26], which is also influenced by particle number fluctuations and the resolution of Ψ_2. That is, stronger CME-driven signals lead to narrower concave-shaped distributions (smaller widths), which are made broader by particle number fluctuations and poorer event-plane resolutions. The influence of the particle number fluctuations can be minimized by scaling ΔS by the width $\sigma_{\Delta_{\rm Sh}}$ of the distribution for $N_{\rm shuffled}(\Delta S)$ *i.e.*, $\Delta S' = \Delta S/\sigma_{\Delta_{\rm Sh}}$. Very little, if any, difference in the event plane resolution for the two isobars, is expected for the centrality range discussed. Therefore, it is not necessary to consider the effects of event plane resolution in the evaluations to obtain the relative charge separation difference.

Figure 3 compares the $R_{\Psi_2}(\Delta S')$ correlators obtained from currently available AVFD events for $^{96}_{40}$Zr + $^{96}_{40}$Zr collisions $^{96}_{44}$Ru + $^{96}_{44}$Ru at $\sqrt{s_{\rm NN}} = 200$ GeV. Panels (a) and (b) show the results for 20-40% and 40-60% central collisions respectively. In each plot, we have scaled ΔS by the width $\sigma_{\Delta S_{\rm Sh}}$, of the $N_{\rm Shuffled}$ distribution, to account for possible differences in the associated number fluctuations due to charge particle multiplicity differences for the isobars at each centrality. The concave-shaped distributions, apparent in each panel, confirm the AVFD

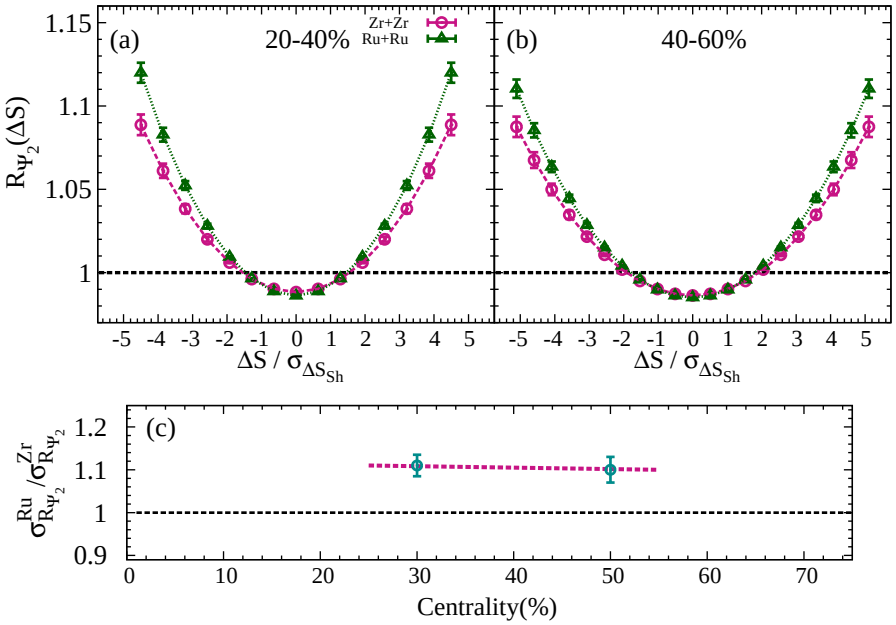

FIG. 3. Comparison of the $R_{\Psi_2}(\Delta S)$ correlators obtained from simulated AVFD events for $^{96}_{40}$Zr + $^{96}_{40}$Zr and $^{96}_{44}$Ru + $^{96}_{44}$Ru at $\sqrt{s_{\rm NN}}$ = 200 GeV, for 20 − 40% (a) and 40 − 60% (b) central collisions. Panel (c) shows the ratio $\sigma_{R^{Zr}_{\Psi_2}}/\sigma_{R^{Ru}_{\Psi_2}}$, of the Gaussian widths extracted from the correlators for the isobars. The magnitude of the charge separation is inversely proportional to the width of the $R_{\Psi_2}(\Delta S)$ correlator.

input CME-driven signal for the isobars. To quantify the isobaric charge separation difference at each centrality, a Gaussian fit (indicated by the curves) was made to the respective correlators in each panel, to extract the associated widths.

The apparent difference in the widths $\sigma_{R_{\Psi_2}}$, of the distributions for $^{96}_{40}$Zr + $^{96}_{40}$Zr and $^{96}_{44}$Ru + $^{96}_{44}$Ru reflects the increase in charge separation expected from the difference in the magnitude of the $\vec{B}$ field for the two isobars. Fig. 3(c) shows the ratio $\sigma_{R^{Zr}_{\Psi_2}}/\sigma_{R^{Ru}_{\Psi_2}}$, for the two centrality selections. They indicate a charge separation which is $\sim 10\%$ larger for $^{96}_{44}$Ru + $^{96}_{44}$Ru as expected from the magnetic field difference. The observed trend with centrality is also consistent with expectation, c.f. Fig.1. The implied sensitivity of these results suggests that the $R_{\Psi_2}(\Delta S)$ correlator would be able to discern and quantify a CME-driven charge separation signal of comparable magnitude, in the upcoming isobaric collisions experiment at RHIC. Here, it is noteworthy that in a recent study [34] the commonly employed Gamma correlator [35–41] was shown to be more strongly influenced by background correlations than the $R_{\Psi_2}(\Delta S)$ correlator.

The relative influence of the background correlations for the two isobars can also be studied directly, via isobaric ratios of the correlation functions:

$$\frac{[C_{\Psi_2}(\Delta S)]_{\rm Ru+Ru}}{[C_{\Psi_2}(\Delta S)]_{\rm Zr+Zr}}, \qquad \frac{[C^{\perp}_{\Psi_2}(\Delta S)]_{\rm Ru+Ru}}{[C^{\perp}_{\Psi_2}(\Delta S)]_{\rm Zr+Zr}}. \tag{6}$$

Here, the essential notion is that, the isobaric ratio of $C_{\Psi_2}(\Delta S)$ should be concave-shaped, due to the stronger CME-driven charge separation in $^{96}_{44}$Ru + $^{96}_{44}$Ru collisions. That is, the stronger CME-driven charge separation for $^{96}_{44}$Ru + $^{96}_{44}$Ru would lead to a narrower width for the $C_{\Psi_2}(\Delta S)$ distribution for the $^{96}_{44}$Ru isobar. In contrast, the isobaric ratio of $C^{\perp}_{\Psi_2}(\Delta S)$, which only measures background-driven charge separation, should be essentially flat due to the expected similarity of the background correlations for the two isobars. A flat distribution would confirm the cancellation of background contributions to the isobaric ratio for $C_{\Psi_2}(\Delta S)$. A deviation from this flat expectation would provide a benchmark for possible differences in background-driven charge separation for the two isobars. Such differences could be cross-checked for collision centralities ($\lesssim 30\%$) where background differences are expected for the two isobars [30]. Note as well that such a background influence could be further checked via comparisons of the $R_{\Psi_3}(\Delta S)$ correlators, since they are insensitive to CME-driven charge separation [26].

The respective isobaric ratios shown in Fig. 4, validate the expected patterns for the CME- and background-driven signals in AVFD events. Note as well that the concavity of the distribution for the $C_{\Psi_2}(\Delta S)$ isobaric ratio, is consistent with $R_{\Psi_2}(\Delta S)$ correlator distributions shown in Fig. 3. The distributions in Fig. 4 constitute an additional cross check for identifying and characterizing the CME-driven charge separation difference for the $^{96}_{40}$Zr + $^{96}_{40}$Zr and $^{96}_{44}$Ru + $^{96}_{44}$Ru isobars, as well as for quantifying the relative influence of their respective

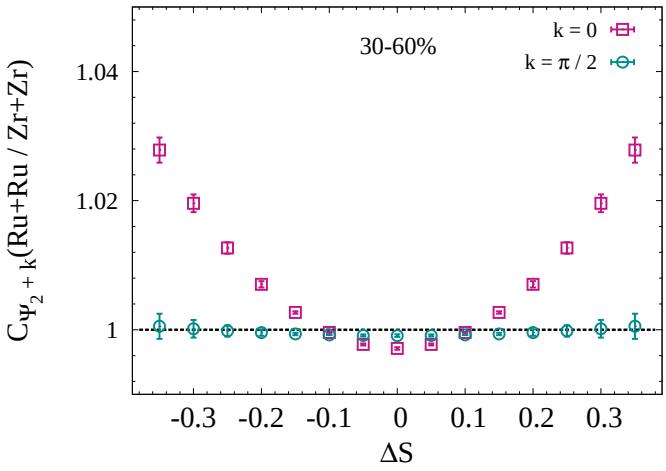

FIG. 4. Comparison of the ratio of the $C_{\Psi_2}(\Delta S)$ correlation functions, used to quantify charge separation parallel to the $\vec{B}$ field for both isobars, and the ratio of the $C^{\perp}_{\Psi_2}(\Delta S)$ correlation function, used to quantify charge separation perpendicular to the $\vec{B}$ field for both isobars.

background correlations.

In summary, we have used our newly developed $R_{\Psi_m}(\Delta S)$ correlator, in concert with state-of-the-art Anomalous Viscous Fluid Dynamics (AVFD) model calculations, to test its efficacy to detect and characterize a Chiral-Magnetically-induced charge separation difference in isobaric collisions of $^{96}_{44}$Ru + $^{96}_{44}$Ru and $^{96}_{40}$Zr + $^{96}_{40}$Zr at $\sqrt{s_{\rm NN}}$ = 200 GeV. The tests indicate a discernible CME-driven difference of $\sim 10\%$ in the presence of realistic non-CME backgrounds. They further indicate that the relative influence of the background correlations, present for each isobar, can be quantified. These results suggest that charge separation measurements for these isobaric species, could serve to further constrain unambiguous identification and characterization of both CME-driven and background-driven charge separation in heavy ion collisions at RHIC. Preparations are currently underway for experimental running at RHIC, as well as the extraction of experimental and theoretical differential $R_{\Psi_m}(\Delta S)$ correlators for the $^{96}_{44}$Ru + $^{96}_{44}$Ru and $^{96}_{40}$Zr + $^{96}_{40}$Zr isobaric species.

ACKNOWLEDGMENTS

This research is supported by the US Department of Energy, Office of Science, Office of Nuclear Physics, under contract DE-FG02-87ER40331.A008 (NM, NA and RL) and by the National Science Foundation under Grant No. PHY-1352368 (SS and JL). The AVFD study is based upon work supported by the U.S. Department of Energy, Office of Science, Office of Nuclear Physics, within the framework of the Beam Energy Scan Theory (BEST) Topical Collaboration.

[1] D. E. Kharzeev, J. Liao, S. A. Voloshin, and G. Wang, "Chiral magnetic and vortical effects in high-energy nuclear collisionsA status report," Prog. Part. Nucl. Phys. **88**, 1–28 (2016), arXiv:1511.04050 [hep-ph].
[2] Volker Koch, Soeren Schlichting, Vladimir Skokov, Paul Sorensen, Jim Thomas, Sergei Voloshin, Gang Wang, and Ho-Ung Yee, "Status of the chiral magnetic effect and collisions of isobars," Chin. Phys. **C41**, 072001 (2017), arXiv:1608.00982 [nucl-th].
[3] Fuqiang Wang, "Effects of Cluster Particle Correlations on Local Parity Violation Observables," Phys. Rev. **C81**, 064902 (2010), arXiv:0911.1482 [nucl-ex].
[4] Adam Bzdak, Volker Koch, and Jinfeng Liao, "Azimuthal correlations from transverse momentum conservation and possible local parity violation," (2010), arXiv:1008.4919 [nucl-th].
[5] Soren Schlichting and Scott Pratt, "Charge conservation at energies available at the BNL Relativistic Heavy Ion Collider and contributions to local parity violation observables," Phys. Rev. **C83**, 014913 (2011), arXiv:1009.4283 [nucl-th].
[6] Berndt Muller and Andreas Schafer, "Charge Fluctuations from the Chiral Magnetic Effect in Nuclear Collisions," (2010), arXiv:1009.1053 [hep-ph].
[7] Jinfeng Liao, Volker Koch, and Adam Bzdak, "On the Charge Separation Effect in Relativistic Heavy Ion Collisions," Phys. Rev. **C82**, 054902 (2010), arXiv:1005.5380 [nucl-th].
[8] Vardan Khachatryan *et al.* (CMS), "Observation of charge-dependent azimuthal correlations in pPb collisions and its implication for the search for the chiral magnetic effect," Submitted to: Phys. Rev. Lett (2016), arXiv:1610.00263 [nucl-ex].
[9] Guy D. Moore and Marcus Tassler, "The Sphaleron Rate in SU(N) Gauge Theory," JHEP **02**, 105 (2011), arXiv:1011.1167 [hep-ph].
[10] M. Mace, S. Schlichting, and R. Venugopalan, "Off-equilibrium sphaleron transitions in the Glasma," Phys. Rev. **D93**, 074036 (2016), arXiv:1601.07342 [hep-ph].
[11] V. Skokov, A. Yu. Illarionov, and V. Toneev, "Estimate of the magnetic field strength in heavy-ion collisions," Int. J. Mod. Phys. **A24**, 5925–5932 (2009), arXiv:0907.1396 [nucl-th].
[12] L. McLerran and V. Skokov, "Comments About the Electromagnetic Field in Heavy-Ion Collisions," Nucl. Phys. **A929**, 184–190 (2014), arXiv:1305.0774 [hep-ph].
[13] Kirill Tuchin, "Electromagnetic field and the chiral magnetic effect in the quark-gluon plasma," Phys. Rev. **C91**, 064902 (2015), arXiv:1411.1363 [hep-ph].
[14] Dmitri Kharzeev, "Parity violation in hot QCD: Why it can happen, and how to look for it,"

Phys. Lett. **B633**, 260–264 (2006), arXiv:hep-ph/0406125.
[15] D. Kharzeev and A. Zhitnitsky, "Charge separation induced by P-odd bubbles in QCD matter," Nucl. Phys. **A797**, 67–79 (2007), arXiv:0706.1026 [hep-ph].
[16] Dmitri E. Kharzeev, Larry D. McLerran, and Harmen J. Warringa, "The Effects of topological charge change in heavy ion collisions: 'Event by event P and CP violation'," Nucl. Phys. **A803**, 227–253 (2008), arXiv:0711.0950 [hep-ph].
[17] Kenji Fukushima, Dmitri E. Kharzeev, and Harmen J. Warringa, "The Chiral Magnetic Effect," Phys. Rev. **D78**, 074033 (2008), arXiv:0808.3382 [hep-ph].
[18] Dmitri E. Kharzeev and Dam T. Son, "Testing the chiral magnetic and chiral vortical effects in heavy ion collisions," Phys. Rev. Lett. **106**, 062301 (2011), arXiv:1010.0038 [hep-ph].
[19] Yin Jiang, Shuzhe Shi, Yi Yin, and Jinfeng Liao, "Quantifying the chiral magnetic effect from anomalous-viscous fluid dynamics," Chin. Phys. **C42**, 011001 (2018), arXiv:1611.04586 [nucl-th].
[20] Dam T. Son and Piotr Surowka, "Hydrodynamics with Triangle Anomalies," Phys. Rev. Lett. **103**, 191601 (2009), arXiv:0906.5044 [hep-th].
[21] Valentin I. Zakharov, "Chiral Magnetic Effect in Hydrodynamic Approximation," (2012), 10.1007/978-3-642-37305-3-11, [Lect. Notes Phys.871,295(2013)], arXiv:1210.2186 [hep-ph].
[22] Kenji Fukushima, "Views of the Chiral Magnetic Effect," Lect. Notes Phys. **871**, 241–259 (2013), arXiv:1209.5064 [hep-ph].
[23] Sandeep Chatterjee and Prithwish Tribedy, "Separation of flow from the chiral magnetic effect in U + U collisions using spectator asymmetry," Phys. Rev. **C92**, 011902 (2015), arXiv:1412.5103 [nucl-th].
[24] The choice of the input model parameters for the two isobars, has a modest influence on the magnitude of the calculated $\vec{B}$-field difference.
[25] Sergei A. Voloshin, "Parity violation in hot QCD: How to detect it," Phys. Rev. **C70**, 057901 (2004), arXiv:hep-ph/0406311 [hep-ph].
[26] Niseem Magdy, Shuzhe Shi, Jinfeng Liao, N. Ajitanand, and Roy A. Lacey, "A New Correlator to Detect and Characterize the Chiral Magnetic Effect," (2017), arXiv:1710.01717 [physics.data-an].
[27] Roy A. Lacey (For the STAR Collaboration), "Charge separation measurements in p(d)+A and A(B)+A collisions: Implications for characterization of the chiral magnetic effect," Fudan University, Shanghai China, 2017, https://indico.cern.ch/event/614524/contributions/2702626/attachments/1513603/2361255/Lacey_QCD-Phases_2017-c.pdf.
[28] Shuzhe Shi, Yin Jiang, Elias Lilleskov, and Jinfeng Liao, "Anomalous Chiral Transport in Heavy Ion Collisions from Anomalous-Viscous Fluid Dynamics," (2017), arXiv:1711.02496 [nucl-th].
[29] Huichao Song, Steffen A. Bass, Ulrich Heinz, Tetsufumi Hirano, and Chun Shen, "200 A GeV Au+Au collisions serve a nearly perfect quark-gluon liquid," Phys. Rev. Lett. **106**, 192301 (2011), [Erratum: Phys. Rev. Lett.109,139904(2012)], arXiv:1011.2783 [nucl-th].
[30] Wei-Tian Deng, Xu-Guang Huang, Guo-Liang Ma, and Gang Wang, "Test the chiral magnetic effect with isobaric collisions," Phys. Rev. **C94**, 041901 (2016), arXiv:1607.04697 [nucl-th].
[31] John Bloczynski, Xu-Guang Huang, Xilin Zhang, and Jinfeng Liao, "Azimuthally fluctuating magnetic field and its impacts on observables in heavy-ion collisions," Phys. Lett. **B718**, 1529–1535 (2013), arXiv:1209.6594 [nucl-th].
[32] D. Kharzeev, A. Krasnitz, and R. Venugopalan, "Anomalous chirality fluctuations in the initial stage of heavy ion collisions and parity odd bubbles," Phys. Lett. **B545**, 298–306 (2002), arXiv:hep-ph/0109253 [hep-ph].
[33] N. N. Ajitanand, Roy A. Lacey, A. Taranenko, and J. M. Alexander, "A New method for the experimental study of topological effects in the quark-gluon plasma," Phys. Rev. **C83**, 011901 (2011), arXiv:1009.5624 [nucl-ex].
[34] Yifeng Sun and Che Ming Ko, "Chiral kinetic approach to the chiral magnetic effect in isobaric collisions," (2018), arXiv:1803.06043 [nucl-th].
[35] B. I. Abelev *et al.* (STAR), "Azimuthal Charged-Particle Correlations and Possible Local Strong Parity Violation," Phys. Rev. Lett. **103**, 251601 (2009), arXiv:0909.1739 [nucl-ex].
[36] B. I. Abelev *et al.* (STAR), "Observation of charge-dependent azimuthal correlations and possible local strong parity violation in heavy ion collisions," Phys. Rev. **C81**, 054908 (2010), arXiv:0909.1717 [nucl-ex].
[37] L. Adamczyk *et al.* (STAR), "Fluctuations of charge separation perpendicular to the event plane and local parity violation in $\sqrt{s_{NN}}$ = 200 GeV Au+Au collisions at the BNL Relativistic Heavy Ion Collider," Phys. Rev. **C88**, 064911 (2013), arXiv:1302.3802 [nucl-ex].
[38] L. Adamczyk *et al.* (STAR), "Measurement of charge multiplicity asymmetry correlations in high-energy nucleus-nucleus collisions at $\sqrt{s_{NN}}$ = 200 GeV," Phys. Rev. **C89**, 044908 (2014), arXiv:1303.0901 [nucl-ex].
[39] L. Adamczyk *et al.* (STAR), "Beam-energy dependence of charge separation along the magnetic field in Au+Au collisions at RHIC," Phys. Rev. Lett. **113**, 052302 (2014), arXiv:1404.1433 [nucl-ex].
[40] Prithwish Tribedy (STAR), "Disentangling flow and signals of Chiral Magnetic Effect in U+U, Au+Au and p+Au collisions," in *Quark Matter 2017, Chicago, Illinois, USA, 2017* (2017) arXiv:1704.03845 [nucl-ex].
[41] Jie Zhao, Hanlin Li, and Fuqiang Wang, "Isolating backgrounds from the chiral magnetic effect," (2017), arXiv:1705.05410 [nucl-ex].